

Hall-conductivity sign change and fluctuations in amorphous $\text{Nb}_x\text{Ge}_{1-x}$ films

Nobuhito Kokubo, Jan Aarts, and Peter H. Kes

Kamerlingh Onnes Laboratory, Leiden University, P. O. Box 9504, 2300 RA Leiden, The Netherlands

(Received 8 December 2000; published 11 June 2001)

The sign change in the Hall conductivity has been studied in thin amorphous $\text{Nb}_{1-x}\text{Ge}_x$ ($x \approx 0.3$) films. By changing the film thickness it is shown that the field at which the sign reversal occurs shifts to lower values (from above to below the mean-field transition field H_{c2}) with increasing film thickness. This effect can be understood in terms of a competition between a positive-normal and a negative-fluctuation contribution to the Hall conductivity.

DOI: 10.1103/PhysRevB.64.014507

PACS number(s): 74.25.Fy, 74.40.+k, 74.80.Bj

I. INTRODUCTION

One of the puzzling and intriguing phenomena in type-II superconductors is the sign change in the Hall effect near the mean-field transition at the upper critical field H_{c2} . Such a Hall anomaly has been observed in some conventional low- T_c superconductors, such as, moderately disordered Nb and V (Ref. 1) and amorphous MoSi (Refs. 2 and 3) and MoGe (Ref. 4) films, as well as most high- T_c superconductors (HTSC).⁵ Hagen *et al.*⁵ pointed out the importance of the electron mean-free path for the Hall anomaly and concluded that very clean and very dirty materials do not show Hall anomalies. However, studies on amorphous dirty superconductors contradict this conclusion.²⁻⁴

Recent phenomenological approaches based on the time-dependent Ginzburg-Landau (TDGL) equation have qualitatively explained the sign anomaly.⁶⁻⁸ In these theories, the sign reversal is just a consequence of the difference in sign between the normal (or quasiparticle) term and the superconducting fluctuation (or vortex flow) term of the Hall conductivity. Several authors⁹⁻¹² have derived the sign of the fluctuation (vortex flow) term from the TDGL equation for BCS superconductors. Recent experimental studies¹³ on HTSC's have pointed out that the sign predictions of these theories are not correct for HTSC's, but they should be valid for BCS superconductors.

Even if the sign of the Hall-fluctuation conductivity were clear, its temperature and field dependence is a matter of discussion. Recent experimental studies on $\text{YBa}_2\text{Cu}_3\text{O}_{7-\delta}$ films¹⁴⁻¹⁶ and single-crystalline $\text{Bi}_2\text{Sr}_2\text{CaCu}_2\text{O}_{8+\delta}$ and $\text{Bi}_{1.95}\text{Sr}_{1.65}\text{La}_{0.4}\text{CuO}_{6+\delta}$ (Ref. 17) have observed that the sign change takes place above H_{c2} , while other studies have claimed that the sign anomaly takes place below H_{c2} . In this problem, the definition of H_{c2} as well as the temperature and field dependence of the Hall-fluctuation conductivity is very important.

As reported in conventional amorphous films¹⁸ as well as HTSC's, the longitudinal conductivity in a perpendicular magnetic field shows a smooth crossover from the paraconducting regime to flux-flow regime around H_{c2} , which is strikingly different from the picture of the conventional fluctuation theory in which the conductivity due to the direct fluctuation contributions of the Aslamazov-Larkin (AL) process diverges at H_{c2} .¹⁹ Thus, it was difficult to define H_{c2} correctly from the fluctuation theory. Recent TDGL

theories,⁶ however, have successfully explained the smooth crossover around H_{c2} by taking into account the interaction term of superconducting fluctuations of the AL process within the Hartree approximation. Later, Ullah and Dorsey (UD) (Ref. 7) developed this further and proposed a scaling theory for the longitudinal and Hall conductivities. This scaling approach is very useful to determine H_{c2} correctly and to describe the field and temperature dependence of the conductivities.

In this paper, we present measurements and analysis of the longitudinal and Hall resistivities ρ_{xx} and ρ_{yx} for thin amorphous (a-) $\text{Nb}_{1-x}\text{Ge}_x$ ($x \approx 0.3$) films ($T_c \approx 3$ K) according to the TDGL theories. We confirm that the smooth crossover in the longitudinal conductivity around H_{c2} is well explained by the UD scaling theory as was found previously,²⁰ and determine H_{c2} . We then show that for the thinner films the sign change in the Hall conductivity takes place above H_{c2} . Contrary to results on HTSC's, we show that the sign of the Hall conductivity is consistent with the TDGL theory for BCS superconductors. We discuss the origin of the sign reversal observed here.

II. EXPERIMENT

The films used in this study were deposited by rf sputtering on Si substrates held at room temperature in a system with a base pressure of 10^{-6} mbar, using 10^{-2} mbar Ar gas as a sputtering gas. The thicknesses used were 16, 34, 60, and 163 nm. X-ray diffraction showed the films to be amorphous. The average composition for each film was determined by electron-microprobe analysis. The distribution in the composition δx is less than 1%. The superconducting mean-field transition temperature in zero field, T_c , was determined from the temperature dependence of resistivity by using the AL fluctuation theory.²¹ From a previous systematic study on *a*- $\text{Nb}_{1-x}\text{Ge}_x$ films,²² the distribution of T_c due to δx is estimated to be less than 18 mK ($\delta T/T_c \lesssim 6 \times 10^{-3}$) around $x = 0.3$. Except for the film thickness, these films have the following identical parameters; the average composition $x \approx 0.3$, $T_c \approx 3$ K, the normal-state resistivity $\rho_{xx}^n \approx 2.2 \mu\Omega\text{m}$, $S \equiv -d(\mu_0 H_{c2})/dT|_{T_c} \approx 2$ T/K, the Ginzburg-Landau (GL) coherence length at $T = 0$ $\xi_{GL}(0) \approx 7.3$ nm, and the GL parameter for dirty limit $\kappa \approx 75$. These films were ion-etched in 200- μm -wide strips with

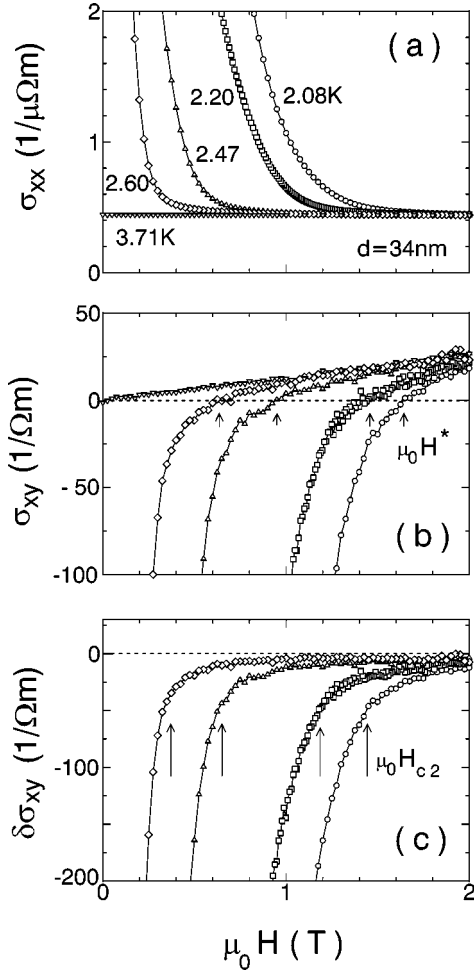


FIG. 1. The field dependence of (a) the longitudinal, (b) Hall, and (c) Hall-fluctuation conductivities at different T of 2.08 K (\circ), 2.20 K (\square), 2.47 K (\triangle), 2.60 K (\diamond), and 3.71 K (∇) for a 34-nm-thick film. The short and long arrows denote the sign-reversal field H^* and the mean-field transition field H_{c2} , respectively.

eight voltage and two current contacts. The longitudinal and Hall resistivities are measured by a conventional dc four-probe method. The longitudinal component due to the misalignment in the Hall probes was subtracted by reversing the field direction. The films are immersed in liquid ^4He to obtain good thermal contact. The magnetic field is normal to the film surface. The normal resistivity ρ_{xx}^n in the temperature range of 1.5 K $< T <$ 5 K has a small temperature coefficient $(\rho_{xx}^n)^{-1} d\rho_{xx}^n/dT \sim -10^{-4} \text{ K}^{-1}$.

III. RESULT AND DISCUSSION

In this study, $\rho_{xx}(=E_x/J_x)$ and $\rho_{yx}(=E_y/J_x)$ were measured as a function of H ($|\mu_0 H| \leq 8 \text{ T}$) at various T . Figures 1(a) and 1(b) show the field dependence of the longitudinal $\sigma_{xx}[\equiv \rho_{xx}/(\rho_{xx}^2 + \rho_{yx}^2)]$ and Hall conductivities $\sigma_{xy}[\equiv \rho_{yx}/(\rho_{xx}^2 + \rho_{yx}^2)]$ at different T for the 34-nm-thick film with $T_c = 2.77 \text{ K}$. To reduce the effect of pinning in the

mixed state, the measuring current density J was selected to be $1.4 \times 10^7 \text{ A/m}^2$ that is much higher than the depinning current density J_c ($\sim 10^5 \text{ A/m}^2$), but smaller than the depairing current density ($\sim 10^{10} \text{ A/m}^2$).

Far above T_c , σ_{xx} is field independent while σ_{xy} is directly proportional to H , that is, the normal-state Hall effect appears. The normal-state Hall conductivity σ_{xy}^n has a positive sign. Within the Drude model, the normal-state Hall angle, $\tan \theta_H^n$, is given by

$$\tan \theta_H^n \equiv \sigma_{xy}^n / \sigma_{xx}^n = \omega_c \tau, \quad (1)$$

where ω_c is the cyclotron frequency and τ is the elastic scattering time of electrons. Compared with typical result on HTSC's ($\omega_c \tau \sim 10^{-2}$ at $\mu_0 H = 1 \text{ T}$), the present films have very small value of $\omega_c \tau \sim 10^{-5}$ at $\mu_0 H = 1 \text{ T}$, indicating the very small mean-free path to be expected for amorphous metals.

Near and below T_c one can clearly see that σ_{xy} changes sign at a certain field H^* in Fig. 1(b). We do not observe any second sign change below H^* , in contrast to what has been reported for several HTSC's.²³ Far above H^* , σ_{xy} recovers the direct proportionality to H and the normal-state Hall effect appears again, indicating that the superconducting fluctuations are completely suppressed by magnetic field. We therefore can define σ_{xy}^n below T_c unambiguously.

In order to determine H_{c2} , we use the UD scaling theory. According to this theory, the longitudinal conductivity is composed of the normal (or quasiparticle) term σ_{xx}^n and superconducting-fluctuation (or vortex-flow) term $\delta\sigma_{xx}$, and expressed as

$$\sigma_{xx} = \sigma_{xx}^n + \delta\sigma_{xx}. \quad (2)$$

$\delta\sigma_{xx}$ interpolates smoothly from the paraconducting regime to flux-flow regime around H_{c2} and obeys universal scaling functions \tilde{F}_{\pm} where $\tilde{F}_{+}(\tilde{F}_{-})$ is the scaling function for $H > H_{c2}(H < H_{c2})$. These functions depend on the dimensionality governed by the ratio of the film thickness d and the length scale ξ for fluctuations of the order parameter near H_{c2} . For the thickness of the films in this study we can apply two-dimensional (2D) scaling functions.²⁰ At each T we identify σ_{xx}^n with σ_{xx} taken at a field (typically 7 T) where σ_{xy} depends linearly on field and σ_{xx} is field independent. $\delta\sigma_{xx}$ is obtained by subtracting σ_{xx}^n from σ_{xx} . Figure 2 shows a typical scaling result. Here, the data are plotted above $H_{c2}(T)/3$ where the lowest Landau level (LLL) approximation for the scaling functions is valid.²⁰ One can clearly see that the scaled longitudinal fluctuation conductivity $\tilde{F}_{xx}^{2D}[\equiv \delta\sigma_{xx}/\{C\sigma_{xx}^n(A_0^{2D}t/h)^{1/2}\}]$ collapses on two universal curves \tilde{F}_{\pm} as a function of the scaled field x^{2D} given by $x^{2D} \equiv \epsilon_H / \sqrt{A_0^{2D}th}$, with $\epsilon_H = \mu_0[H - H_{c2}(T)]/ST_c$, although deviations are visible at large $|x^{2D}|$. Here, $t = T/T_c$ and $h = \mu_0 H/ST_c$ are normalized temperature and field, respectively. C is related to the real part of the relaxation time of the order parameter $\gamma = \gamma_1 + i\gamma_2$. We take a dirty limit value of $C = 1.447$.²⁰ The strength of thermal fluctuations for 2D system, A_0^{2D} , is given by $A_0^{2D} = 4\sqrt{2}G_i\xi_{GL}(0)/d$ where

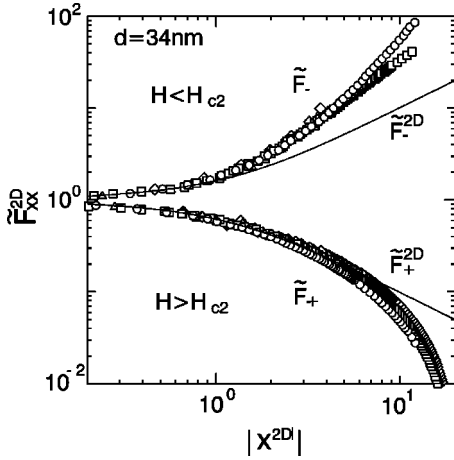


FIG. 2. The scaled fluctuation conductivity plotted as a function of $|x^{2D}|$ at different T of 2.08 K, 2.20 K, 2.47 K, and 2.60 K. The current density J is 2.94×10^7 A/m² except for the curve at 2.08 K where $J = 1.47 \times 10^7$ A/m². The symbols correspond to those in Fig. 1. The solid curves represent the 2D universal scaling functions \tilde{F}_{\pm}^{2D} . S is found to be 2.16 from the scaling collapse of the data taken at 2.47 K and 2.60 K close to $T_c = 2.77$ K. The H_{c2} values for 2.08 K and 2.20 K are determined from the scaling collapse of the data using this S value.

$G_i (\approx 5 \times 10^{-6})$ is the Ginzburg number.²⁴ Very close to H_{c2} , deviations due to the inhomogeneity in the composition δx become apparent. Hence, we do not plot the data in fields $|\epsilon_H| < (1/2) \delta T_c / T_c \approx 3 \times 10^{-3}$, which roughly corresponds to $|x^{2D}| < 0.2$. In such a scaling plot, the unknown parameters are S and $H_{c2}(T)$. In the temperature range close to T_c , they are connected by the simple relation $H_{c2}(T) = S(T_c - T)$. We first determine S from the scaling collapse of the data close to T_c and this S value is used to determine H_{c2} far below T_c in the scaling analysis. Thus, we can unambiguously determine H_{c2} from the scaling collapse of the data.

Before proceeding to the result of the H_{c2} line, we compare the scaling functions \tilde{F}_{\pm} with those predicted in the UD theory. The UD theory implies that the 2D universal functions \tilde{F}_{\pm}^{2D} in the high-field limit are given by

$$x^{2D} = 1/\tilde{F}^{2D} - \tilde{F}^{2D}, \quad (3)$$

if the pinning effect in the flux-flow regime is negligible and the fluctuation conductivity in the paraconducting regime is dominated by the direct fluctuation contributions of the AL process. These functions are applicable to the field range where the LLL is satisfied. The solid lines in Fig. 2(a) denote these universal functions. \tilde{F}_{\pm} agrees well with \tilde{F}_{\pm}^{2D} near H_{c2} ($-1 \leq x_{2D} \leq 6$), while deviations are visible in the large $|x^{2D}|$ regime. In the paraconducting regime, \tilde{F}_{+} decreases much faster than \tilde{F}_{+}^{2D} above $x^{2D} \approx 6$. Such a rapid decrease in $\delta\sigma_{xx}$ was also observed far above H_{c2} in amorphous thick films and attributed qualitatively to a phenomenological short-wavelength cutoff in the fluctuation spectrum.²⁵ For the other films ($d = 16$ and 60 nm) except for the thickest film ($d = 163$ nm),²⁶ similar deviation of \tilde{F}_{+} begins to appear at

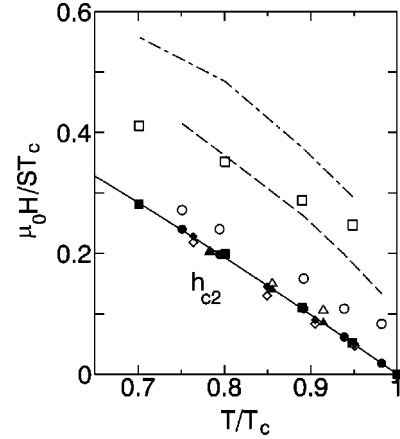


FIG. 3. $\mu_0 H_{c2} / ST_c$ plotted as a function of T/T_c for different films of 16 nm (■), 34 nm (●), 60 nm (▲), and 163 nm (◆) thickness. The solid curve represents the mean-field line in the dirty limit for the WHH theory. The corresponding open symbols show $\mu_0 H^* / ST_c$ for the same films plotted against T/T_c . The dashed and dashed-dotted lines represent the phenomenological boundaries (given in text) for 34-nm- and 16-nm-thick films, respectively. For clarity, the boundary for 60 nm is not shown.

almost the same value of $x^{2D} \approx 6$, although the physical origin of the short-wavelength cutoff is not clear. The definition of σ_{xx}^n does not affect this behavior because the field at which σ_{xx}^n is defined is much larger than the fields of interest. Hereafter, we regard $x^{2D} = 6$ as the phenomenological boundary below which $\delta\sigma_{xx}$ is well described by the UD scaling theory, and discuss our data below this boundary.

From the scaling collapse of $\delta\sigma_{xx}$ we obtained the H_{c2} line for films with different thicknesses. To compare those results, we plot the normalized mean-field value of $\mu_0 H_{c2} / ST_c (\equiv h_{c2})$ against normalized temperature T/T_c for different films in Fig. 3. Good agreement is seen for H_{c2} of all films. The solid line represents the mean-field line for the dirty limit in the Werthamer-Helfand-Hohenberg (WHH) theory, which is given by

$$\ln(t) = \Psi(1/2) - \Psi[1/2 + (2/\pi^2)h_{c2}/t], \quad (4)$$

where Ψ is the digamma function.²⁷ The H_{c2} line obtained is well approximated by this relation, giving experimental support for the validity of the UD scaling theory.

Next, we turn to results of the Hall-fluctuation conductivity. In the TDGL theories,⁷ the Hall conductivity also consists of a normal (or quasiparticle) term and a superconducting fluctuation (or vortex flow) term,

$$\sigma_{xy}(H, T) = \sigma_{xy}^n(H, T) + \delta\sigma_{xy}(H, T). \quad (5)$$

Hence, we subtract $\sigma_{xy}^n(H, T)$ from $\sigma_{xy}(H, T)$, and plot $\delta\sigma_{xy}(H, T)$ against H in Fig. 1(c). The plot shows that $\delta\sigma_{xy}$ always has a negative sign. H_{c2} is denoted by the long arrows. With decreasing H the magnitude of $\delta\sigma_{xy}$ increases monotonically and grows as $1/H$ at low H ($\ll H_{c2}$) (not shown) as the TDGL theories predict.²⁸ Thus, the sign reversal of σ_{xy} at H^* always takes place when $\delta\sigma_{xy}$ and σ_{xy}^n are different in sign. Beforehand it is not clear whether or not

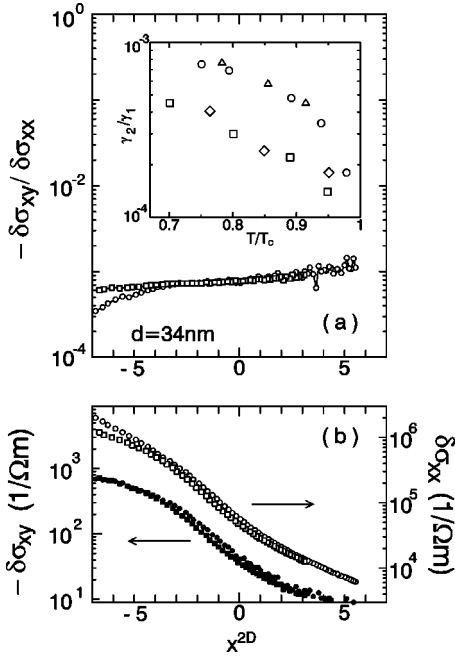


FIG. 4. (a) The ratio of the fluctuation conductivities, $-\delta\sigma_{xy}/\delta\sigma_{xx}$, plotted as a function of x^{2D} at $T=2.08$ K for the 34-nm-thick film with different J of 1.4 kA/cm² (○) and 4.4 kA/cm² (□). (b) The corresponding longitudinal (○, □) and Hall fluctuation conductivities (●, ■) are also plotted as a function of x^{2D} with different J . Inset in (a) shows the T/T_c dependence of $\gamma_2/\gamma_1 (= -\delta\sigma_{xy}/\delta\sigma_{xx})$ at H_{c2} with different thickness of 16 nm (□), 34 nm (○), 60 nm (△), and 163 nm (◇).

H^* is above H_{c2} , because σ_{xy}^n and $\delta\sigma_{xy}$ depend in different ways on the electronic structure of the material. As one can see in Fig. 3, in the thinnest film H^* (denoted by open symbols) is always above H_{c2} but below the phenomenological boundary where scaling analysis starts to fail. It may be worth pointing out that H^* decreases monotonically with rising T and terminates finally at a certain T^* above T_{c0} in zero field. With increasing d , H^* moves systematically closer to H_{c2} and it finally shifts below (but very close to) H_{c2} for the thickest film, implying that the contribution of the negative $\delta\sigma_{xy}$ to positive σ_{xy}^n decreases with increasing d . These results support the view that enhancing the superconducting fluctuations by reducing d leads to an increasing negative Hall conductivity working against positive σ_{xy}^n , which is responsible for the sign reversal above H_{c2} .

We now discuss the field and temperature dependences of $\delta\sigma_{xy}$, in comparison with the UD scaling theory. According to this theory, $\delta\sigma_{xx}$ and $\delta\sigma_{xy}$ have the same field and temperature dependence and their ratio should be independent of H and T . Note that $\delta\sigma_{xy}/\delta\sigma_{xx} = -\gamma_2/\gamma_1$, the ratio of the imaginary and real part of γ .⁷ We did not find scaling of $\delta\sigma_{xy}$. A recent study on YBa₂Cu₃O_{7- δ} films¹⁴ has pointed out that the failure of the scaling of $\delta\sigma_{xy}$ can be attributed to the additional contributions of the Maki-Thompson (MT) process, which are not taken into account in the UD theory. However, the MT process cannot explain the present result because the strong pair-breaking effect in the amorphous dirty films should lead to a small contribution.^{25,29} As one

can see in the inset of Fig. 4(a), contrary to the UD scaling theory, $-\delta\sigma_{xy}/\delta\sigma_{xx}$ at H_{c2} increases monotonically with cooling. Similar temperature dependence of $-\delta\sigma_{xy}/\delta\sigma_{xx}$ has been reported for amorphous MoSi films.³ We conclude that the main reason for the scaling failure is the temperature dependence of γ_2/γ_1 . Further microscopic calculations based on the BCS theory are required to explain this effect.

The field dependence of $-\delta\sigma_{xy}/\delta\sigma_{xx}$ is shown in Fig. 4(a) for two current densities. In the field range ($-1 \leq x^{2D} \leq 6$) where $\delta\sigma_{xx}$ follows the UD scaling theory, $-\delta\sigma_{xy}/\delta\sigma_{xx}$ is independent of J and depends only weakly on x^{2D} . As one can see in Fig. 4(b), however, in the same field range both conductivities change almost one decade in magnitude and their dependences on x^{2D} look very similar. Hence, we believe that both $\delta\sigma_{xx}$ and $\delta\sigma_{xy}$ in the paraconducting regime ($0 \leq x^{2D} \leq 6$) are dominated by the direct fluctuation contributions of the AL process and thus the contributions of the AL process are responsible for the sign change of the Hall conductivity above H_{c2} .

Finally, we discuss the origin of the sign in σ_{xy}^n and $\delta\sigma_{xy}$ for our amorphous films. The sign of σ_{xy}^n depends on the sign of the group velocity $v [= (1/\hbar)\partial\varepsilon/\partial k]$ of electrons at the Fermi level where ε is the energy and k is the wave number. Because of the absence of band structure, the amorphous materials are generally more free-electron-like than their crystalline counterparts. Therefore, the simple amorphous metals generally have negative σ_{xy}^n because of a positive group velocity ($v \propto k > 0$).³⁰ Most of the amorphous transition metals (TM's), however, have positive σ_{xy}^n .³¹ The origin of this positive σ_{xy}^n has been attributed to the s - d hybridization interaction in the TM, which leads to a negative group velocity ($\partial\varepsilon/\partial k < 0$) at the Fermi level if the Fermi energy ε_F lies within the d band.³¹⁻³³ The TM-metalloid-type amorphous superconductors NbGe as well as MoGe and MoSi belong to amorphous TM's and have positive σ_{xy}^n .

In the TDGL theory based on BCS superconductors by Nishio and Ebisawa,¹⁰ the sign of $\delta\sigma_{xy}$ is determined by the electron-hole asymmetry, i.e., by the sign of $-N'$, where $N' [= dN(\varepsilon)/d\varepsilon|_{\varepsilon=\varepsilon_F}]$ is the energy derivative of the density of states (DOS) $N(\varepsilon)$ at the Fermi energy. Numerical calculations of the DOS for, e.g., amorphous Ni imply³² that the total DOS near ε_F is dominated by the DOS for the d band whose energy dependence is characterized by a peak near the center of d -band ε_d and roughly approximated by a parabolic energy dependence with negative curvature, i.e., $N(\varepsilon) \propto -(\varepsilon - \varepsilon_d)^2$. Similar energy dependences of the total DOS have been commonly observed for various amorphous TM-metalloid alloys by photoemission experiments.³⁴ Because Nb is a less than half-filled $4d$ -band metal, ε_F lies below the center of the $4d$ -band ε_{4d} . Thus, a -NbGe films have positive N' . The same argument holds for a -MoGe and MoSi, since Mo is also a less than half-filled $4d$ -band metal. Thus, $\text{sgn}(\delta\sigma_{xy}) = \text{sgn}(-N') < 0$ in both a -NbGe, a -MoGe, and a -MoSi films.²⁻⁴ These findings give experimental support for the prediction of the sign of $\delta\sigma_{xy}$ in the TDGL theory for BCS superconductors.

IV. SUMMARY

In summary, we have measured the longitudinal and Hall resistivities for thin films of the dirty superconductor $a\text{-Nb}_{1-x}\text{Ge}_x$ ($x \approx 0.3$) near H_{c2} . We confirm that $\delta\sigma_{xx}$ obeys the 2D scaling functions of the UD fluctuation theory. We find a good agreement of the obtained H_{c2} line with the WHH theory, supporting the scaling procedure. The failure of the scaling collapse of $\delta\sigma_{xy}$ is attributed to the temperature dependence of γ_2/γ_1 . The Hall conductivity σ_{xy} in thinner films shows a sign change at a certain H^* that is above H_{c2} but in the regime where σ_{xx} follows the UD theory. With increasing film thickness, H^* moves closer to H_{c2} and it finally shifts below (but close to) H_{c2} for the thickest film. The negative contribution of the superconducting fluctuations of the AL process working against positive σ_{xy}^n is re-

sponsible for the sign change above H_{c2} . The negative sign of $\delta\sigma_{xy}$ in the present films is consistent with the electron-hole asymmetry in the framework of the TDGL theory for BCS superconductors.

ACKNOWLEDGMENTS

We are very grateful to R. Ikeda for useful comments and sending us his manuscripts. We would like to thank Y. Matsuda for giving us a copy of his unpublished work. We acknowledge the experimental assistance of R. Besseling, M.B.S. Hesselberth, G.L.E. van Vliet, R.W.A. Hendriks, and T.J. Gortenmulder. This work was part of the research program of the ‘‘Stichting voor Fundamenteel Onderzoek der Materie’’ (FOM), which is financially supported by NWO. One of the authors (N.K.) was financially supported by JSPS.

-
- ¹K. Noto, S. Shinzawa, and Y. Muto, *Solid State Commun.* **18**, 1081 (1976).
²A.W. Smith, T.W. Clinton, C.C. Tsuei, and C.J. Lobb, *Phys. Rev. B* **49**, 12 927 (1994).
³A.W. Smith, T.W. Clinton, W. Liu, C.C. Tsuei, A. Pique, Q. Li, and C.J. Lobb, *Phys. Rev. B* **56**, 2944 (1997).
⁴J.M. Graybeal, J. Luo, and W.R. White, *Phys. Rev. B* **49**, 12 923 (1994).
⁵S.J. Hagen, A.W. Smith, M. Rajeswari, J.L. Peng, Z.Y. Li, R.L. Greene, S.N. Mao, X.X. Xi, S. Bhattacharya, Qi Li, C.J. Lobb, *Phys. Rev. B* **47**, 1064 (1993).
⁶R. Ikeda, T. Ohmi, and T. Tsuneto, *J. Phys. Soc. Jpn.* **58**, 1377 (1989); **59**, 1397 (1990); **60**, 1051 (1991).
⁷S. Ullah and A.T. Dorsey, *Phys. Rev. B* **44**, 262 (1991).
⁸N.V. Kopnin and A.V. Lopatin, *Phys. Rev. B* **51**, 15 291 (1995).
⁹H. Fukuyama, H. Ebisawa, and T. Tsuzuki, *Prog. Theor. Phys.* **46**, 1028 (1971).
¹⁰T. Nishio and H. Ebisawa, *Physica C* **290**, 43 (1997).
¹¹A.G. Arnov and A.B. Rapoport, *Mod. Phys. Lett. B* **6**, 1083 (1992); A.G. Arnov, S. Hikami, and A.L. Larkin, *Phys. Rev. B* **51**, 3880 (1995).
¹²A. van Otterlo, M. Feigel'man, V. Geshkenbein, and G. Blatter, *Phys. Rev. Lett.* **75**, 3736 (1995); M.V. Feigel'man, V.B. Geshkenbein, A.I. Larkin, and V.M. Vinokur, *Pis'ma Zh. Éksp. Teor. Fiz.* **62**, 811 (1995) [*JETP Lett.* **62**, 834 (1995)]; D.I. Khomskii and A. Freimuth, *Phys. Rev. Lett.* **75**, 1384 (1995).
¹³T. Nagaoka, Y. Matsuda, H. Obara, A. Sawa, T. Terashima, I. Chong, M. Takano, and M. Suzuki, *Phys. Rev. Lett.* **80**, 3594 (1998).
¹⁴W. Liu, T.W. Clinton, A.W. Smith, and C.J. Lobb, *Phys. Rev. B* **55**, 11 802 (1997).
¹⁵A.V. Samoilov, *Phys. Rev. B* **49**, 1246 (1994).
¹⁶W. Lang, G. Heine, P. Schwab, X. Z. Wang, and D. Bäuerle, *Phys. Rev. B* **49**, 4209 (1994).
¹⁷R. Jin and H.R. Ott, *Phys. Rev. B* **53**, 9406 (1996).
¹⁸P. Berghuis and P.H. Kes, *Phys. Rev. B* **47**, 262 (1992).
¹⁹For example, K. Maki, *J. Low Temp. Phys.* **1**, 513 (1969).
²⁰M.H. Theunissen and P.H. Kes, *Phys. Rev. B* **55**, 15 183 (1997).
²¹L.G. Aslamazov and A.I. Larkin, *Phys. Lett.* **26A**, 238 (1968).
²²R. Wördenweber, A. Pruyboom, and P.H. Kes, *J. Low Temp. Phys.* **70**, 253 (1987).
²³For example, W.N. Kang, B.W. Kang, Q.Y. Chen, J.Z. Wu, S.H. Yun, A. Gapud, J.Z. Qu, W.K. Chu, D.K. Christen, R. Kerchner, and S.W. Chu, *Phys. Rev. B* **59**, 9031 (1999).
²⁴C.J. Lobb, *Phys. Rev. B* **36**, 3930 (1987).
²⁵W.L. Johnson, C.C. Tsuei, and P. Chaudhari, *Phys. Rev. B* **17**, 2884 (1978).
²⁶The deviations from the 2D scaling functions observed for the thickest film are different from those observed for the thinner films. With increasing $x^{2D} \tilde{F}_+$ for the thickest film exhibits much slower decrease than \tilde{F}_+^{2D} . This stems from the dimensional crossover, although the 3D limit analysis is not fully valid yet (Ref. 20). We believe that for the thickest film the 2D scaling analysis is still valid in a narrow field range near H_{c2} . H_{c2} obtained from the 2D scaling analysis is plotted in Fig. 3.
²⁷N. Werthamer, E. Helfand, and P.C. Hohenberg, *Phys. Rev.* **147**, 295 (1966).
²⁸A.T. Dorsey, *Phys. Rev. B* **46**, 8376 (1992); R.T. Troy and A.T. Dorsey, *ibid.* **47**, 2715 (1993).
²⁹W.F. Skocpol and M. Tinkham, *Rep. Prog. Phys.* **38**, 1049 (1975).
³⁰U. Mizutani, *Prog. Mater. Sci.* **28**, 97 (1983).
³¹B.L. Gallagher, D. Greig, M. A. Howson, and A.A.M. Croxon, *J. Phys. F: Met. Phys.* **13**, 119 (1983).
³²G.F. Weir, M.A. Howson, B.L. Gallagher, and G.J. Morgan, *Philos. Mag. B* **47**, 163 (1983); G.J. Morgan and G.F. Weir, *ibid.* **47**, 177 (1983).
³³G.F. Weir and G.J. Morgan, *J. Phys. F: Met. Phys.* **11**, 1833 (1981).
³⁴W.L. Jonson, *J. Appl. Phys.* **50**, 1557 (1979); B. Schröder, W. Grobman, W.L. Johnson, C.C. Tsuei, and P. Chaudhari, *Solid State Commun.* **28**, 631 (1978); K. Tanaka, M. Yoshino, and K. Suzuki, *J. Phys. Soc. Jpn.* **51**, 3882 (1982); K. Tamura, J. Fukushima, H. Endo, K. Kishi, S. Ikeda, and S. Minomura, *ibid.* **36**, 565 (1974).